JTTEE5 20:160–169
DOI: 10.1007/s11666-010-9591-z
1059-9630/$19.00 © ASM International

Influence of Deposition Temperature on the Microstructures and Properties of Plasma-Sprayed Al_2O_3 Coatings

Shun Hao, Chang-Jiu Li, and Guan-Jun Yang

(Submitted May 14, 2010; in revised form September 3, 2010)

Al_2O_3 coatings were deposited on 1Cr13 substrates by atmospheric plasma spraying at different deposition temperatures of 140, 275, 375, 480, 530, and 660 °C to investigate the effect of coating surface temperature on the lamellar bonding formation. The fractured cross section morphology was characterized by scanning electron microscopy to reveal the lamellar interface bonding. X-ray diffraction was used to characterize the phase contents in the coating. Micro-hardness, Young's modulus, and thermal conductivity of the deposits were measured for examining the dependency of coating properties on its microstructure. The results show that the interface area bonded through columnar grain growth across splat-splat interfaces was increased with increasing deposition temperature. Moreover, micro-hardness, Young's modulus and thermal conductivity were increased with the increase of deposition temperature. However, the phase structure of the coating changed little with deposition temperature. The results evidently indicate that the apparent bonding ratio and properties of deposits can be significantly changed in a wider range through controlling the deposition temperature.

Keywords alumina, deposition temperature, interface bonding, microstructure, plasma spraying, property

1. Introduction

A thermally sprayed deposit is formed by a stream of molten droplets impacting on a substrate followed by flattening, rapid cooling, and solidification processes. The individual droplets spread out to thin lamellae, the stacking of which constitutes the deposit (Ref 1, 2). Atmospheric plasma spraying (APS), due to its relatively high deposition efficiency, flexibility, and easy automation, has become a popular process to produce various protective coatings, such as thermal barrier (Ref 3), wear-resistant (Ref 4), corrosion-resistant (Ref 5), and dielectric coating layers (Ref 6).

This article is an invited paper selected from presentations at the 2010 International Thermal Spray Conference and has been expanded from the original presentation. It is simultaneously published in *Thermal Spray: Global Solutions for Future Applications, Proceedings of the 2010 International Thermal Spray Conference*, Singapore, May 3-5, 2010, Basil R. Marple, Arvind Agarwal, Margaret M. Hyland, Yuk-Chiu Lau, Chang-Jiu Li, Rogerio S. Lima, and Ghislain Montavon, Ed., ASM International, Materials Park, OH, 2011.

Shun Hao, Chang-Jiu Li, and **Guan-Jun Yang**, State Key Laboratory for Mechanical Behavior of Materials, School of Materials Science and Engineering, Xi'an Jiaotong University, Xi'an 710049, ShaanxiPeople's Republic of China. Contact e-mail: licj@mail.xjtu.edu.cn.

Generally, the choice of coating materials for a certain application is determined by their performances. On the other hand, the properties of materials are generally sensitive functions of their microstructures. Therefore, it is a focal point in the research of thermal spraying field to develop coating microstructures and establish the relationships between coating microstructures and properties.

According to the previous investigations (Ref 7-9), plasma-sprayed ceramic deposits exhibit a lamellar structure with limited interface bonding. Voids are present in the deposits, which consist of large 3D and 2D voids corresponding to the nonbonded interface areas and vertical cracks in individual ceramic splats. The previous studies revealed that the lamellar structure with a limited lamellar interface bonding determines the physical and mechanical properties of thermal spray deposits. Moreover, the bonding ratio between adjacent lamellae dominates coating properties (Ref 9). Accordingly, the control of coating properties and subsequently performances should be primarily made through development of lamellae interface bonding. According to quantitative characterization of lamellar structure using the copper electroplating technique, the mean bonding ratio at the lamellar interfaces of Al_2O_3 coating deposited following conventional fashion is less than one-third of the total apparent interface area in the coating (Ref 7-9). The limited bonding ratio of thermally sprayed deposits leads to lower hardness (Ref 10), lower elastic modulus (Ref 11-13), lower fracture toughness (Ref 14), and lower thermal conductivity (Ref 15) than corresponding bulk materials. Consequently, the applications of thermally sprayed coatings will be limited by such feature. Therefore, many investigations have been carried out to understand the

factors determining coating microstructure and in particular the bonding at the interface between lamellae within the deposit (Ref 7-9, 16, 17).

The optimization of coating deposition conditions is usually employed through changing spray particle parameters such as velocity and temperature to modify coating microstructure (Ref 18-20). The substrate temperature is also employed to improve coating adhesion, coating microstructure and properties (Ref 21-23). Most investigations involving the effect of substrate temperature were performed at the temperatures less than about 350 °C which were associated with the transition of splat morphology (Ref 23). In fact, several previous investigations were involved in the coating deposition at much high temperature, the results of which suggested the formation of the coatings with well-bonded lamellar interfaces throughout a thick layer of coating (Ref 24-29). Those investigations were more oriented for development of α-Al_2O_3 in plasma-sprayed Al_2O_3 coating (Ref 24) or segmental cracks in YSZ coatings (Ref 26-29). However, although based on those results reported it could be considered that the coating consisting of well-bonded lamellae can be deposited when droplets are projected on a substrate surface at certain high temperature, few investigations were involved in the effect of coating surface temperature or substrate temperature on the lamellar bonding formation. Recently, it was evidently revealed using YSZ deposits that through the control of substrate temperature, the bonding ratio and subsequently the coating properties can be significantly changed (Ref 17, 30). During deposition, the substrate temperature, especially the coating surface temperature prior to droplet impact can be considered to be a key factor, which influences the deposition characteristic of the molten droplets and bonding of the splat to the prior deposited coating, and subsequently influences the properties of deposited coating. In this paper, the coating surface temperature prior to droplet impact is referred to as the deposition temperature. Up to now, the influence of the deposition temperature on the microstructures and properties of thermally sprayed alumina coatings has not been systematically investigated. However, because thermally sprayed ceramic coatings can possibly be applied to different applications such as thermal barrier coating and wear-resistant coating which typically require porous and dense microstructure, respectively, it is necessary to examine the influence of coating surface temperature on the coating microstructure and subsequently properties to control the properties of the coating through coating surface temperature for different applications. Moreover, the systematical investigation may benefit the understanding of the formation mechanism of the lamellar bonding during splat depositions.

In this study, the influence of the deposition temperature on plasma-sprayed Al_2O_3 coating microstructures was investigated with the emphasis on the examination of the effect of the deposition temperature on lamellar interface bonding and the changes of coating properties accordingly with coating microstructures.

2. Experimental

A fuse-crushed Al_2O_3 powder was used as the feedstock. The particle size range is 25-58 μm. The powder exhibits an angular morphology as shown in Fig. 1(a). The x-ray diffraction (XRD) pattern of the powder is shown in Fig. 1(b). The powder mainly consists of 99.25% α-Al_2O_3 and a trace of β-Al_2O_3 ($Na_2O{\cdot}11Al_2O_3$) based on the XRD analysis.

Al_2O_3 coating was deposited by a commercial plasma spray system (80 kW class). The plasma torch was operated at 39 kW to generate an Ar-H_2 plasma jet. The pressures of primary gas Ar and secondary gas H_2 were fixed at 0.85 and 0.4 MPa, respectively. The flow rates of Ar and H_2 were 54 and 6.6 L/min, respectively. The powder was fed into a plasma jet using an internal powder port to ensure sufficient melting of spray powder particles. The torch-substrate distance during deposition was 80 mm. A robot was used to drive the plasma torch back and forth across the substrate surface. The stainless steel (1Cr13) was used as the substrate.

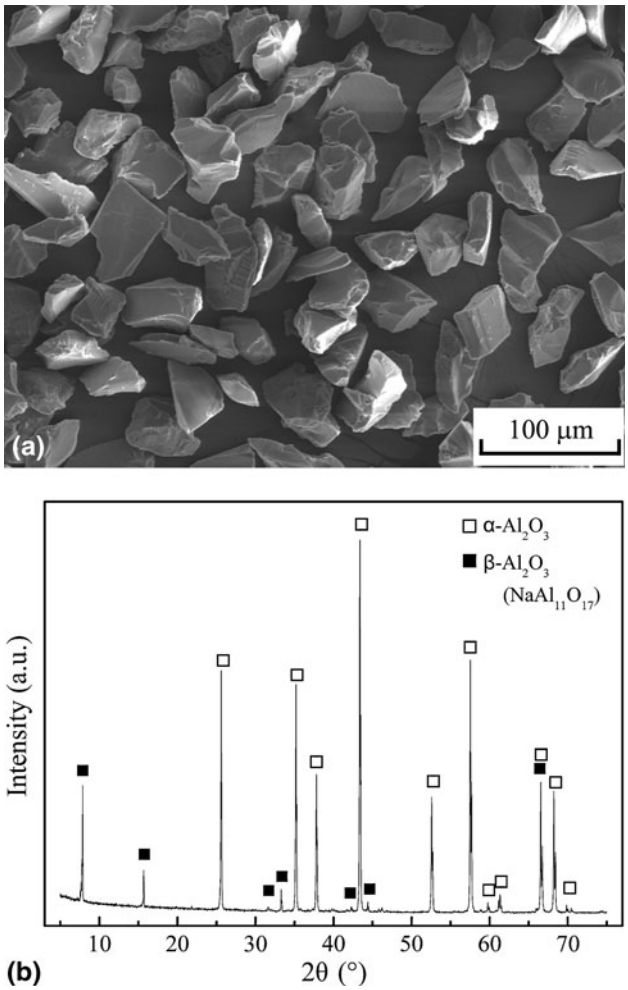

Fig. 1 (a) SEM morphology and (b) XRD pattern of Al_2O_3 powder employed for spraying

Before deposition, the substrate was sand-blasted and preheated to different temperatures by a gas flame torch directing to the back of it. The substrate (or previously deposited coating) surface temperature was monitored using a pyrometer (RAYPM30L3U, Raytek, Santa Cruz, CA, USA). An air jet attached to the torch and oriented toward the substrate was also employed to control the surface temperature by cooling down the substrate and the coating along with the gas flame, when the surface temperature became higher than the given one. The surface temperature ranges of different samples during deposition are shown in Table 1. The mean temperature was used as a parameter to represent the deposition temperature.

Because from a polished cross section of the coating no useful information on the lamellar interface bonding could be observed, the as-sprayed coatings were fractured at a direction perpendicular to the coating surface. The advantage using a fracture surface is that the nonbonded interface or/and weakly bonded interface can be delineated visually under direct observation. Thus, the surface morphologies of fractured coatings were examined by scanning electron microscopy (SEM) to investigate the effect of the deposition temperature on the lamellae interface bonding. Moreover, the polished cross sections of the coatings were also prepared following conventional routine for metallographical analysis, such as cutting, mounting, and polishing, focusing on the change of coating porosity with the coating surface temperature. The coating porosity was estimated through processing of cross-sectional images. Due to inevitable pull-out of loosely bonded particle fractions during polishing of the samples, the porosity was referred to as the apparent porosity. The change of the porosity value could be also considered as an indication of the change of the lamellar bonding with the deposition condition because the pull-outs can be reduced with the improvement of lamellar bonding.

The phases of the coatings were characterized by XRD. The XRD measurement was carried out using Cu Ka radiation. The phase content in the powder and coating was estimated based on the relative intensity ratio (RIR) method (Ref 31, 32), which can be calculated as follows:

$$W_X = \frac{I_{Xi}}{K_A^X \sum_{i=A}^{N} \frac{I_i}{K_A^i}} \quad \text{(Eq 1)}$$

where W_X is the content of phase X, and I is the intensity, and ${K_A}^X$ is the RIR value of phase X and A.

Table 1 Ranges of coating surface temperature during deposition and the mean deposition temperature

Temperature range during deposition, °C	Deposition temperature
80-200	140
250-300	275
350-400	375
450-510	480
520-540	530
620-700	660

Vickers micro-hardness of the coating was measured on a polished cross section at a load of 300 gf and a loading time of 30 s. Young's modulus was measured through the Knoop indentation approach as proposed in literature (Ref 33, 34) at a load of 1000 gf and a loading time of 50 s. Thermal conductivity was measured through the laser flash method (NETZSCH LFA 427) at a temperature range from 25 to 1200 °C. The samples used for thermal conductivity measurement were circular free-standing coating of about 1 mm thick in a diameter of 12.7 mm, which were plasma-sprayed at different deposition temperatures of 153, 302, 515 and 756 °C.

3. Results and Discussion

3.1 Microstructures of Al_2O_3 Coatings

To reveal the lamellae interface bonding, the surface morphology of fractured coatings was examined instead of polished cross-sectional microstructure. Figure 2 shows the typical surface morphology of the cross sections of the fractured coatings deposited at different temperatures. It can be seen that the coatings deposited at lower temperatures exhibit a typical lamellar structure (Fig. 2a, b). The thickness of individual splats corresponding to a single lamella is typically 1 to 2 μm. The columnar grain structure was clearly observed in individual lamellae. Evidently, the limited bonding was present at the interfaces between lamellae. Those facts are well consistent with the previously reported results (Ref 7, 11). When the deposition temperature was increased to a temperature of 480 °C (Fig. 2c-d), the lamellar structure feature, being distinguished by the limited lamellar interface bonding, became less typical. On the other hand, it can be clearly recognized that the columnar grain structure typically in individual splats of thermal spray coating grew across multiples of splats in a direction perpendicular to the lamellar plane, which makes individual splats less distinguishable. This fact is attributed to the increased lamella interface bonding with the increase of the deposition temperature. Evidently, at a temperature higher than 480 °C, most splats were well bonded together through the growth of columnar grains across interfaces (Fig. 2d, g). Moreover, the interface area with columnar grain growth across splat-splat interfaces was increased with increasing deposition temperature. With the increase of the temperature further to 530 and 660 °C (Fig. 2e, f), it was clearly observed that more splats were well bonded together. The above results indicate qualitatively that the lamellar bonding was significantly improved with the increase of coating surface temperature when the mean deposition temperature was increased to the values from 375 to 480 °C. Compared with the deposition temperature of 800 to 900 °C for plasma spraying of YSZ to enhance the significant columnar grain growth across multi-splats reported previously (Ref 17, 35), the above-mentioned temperature observed for alumina deposition is about 400 °C lower than YSZ. It can be considered that the difference of such temperature should depend on the

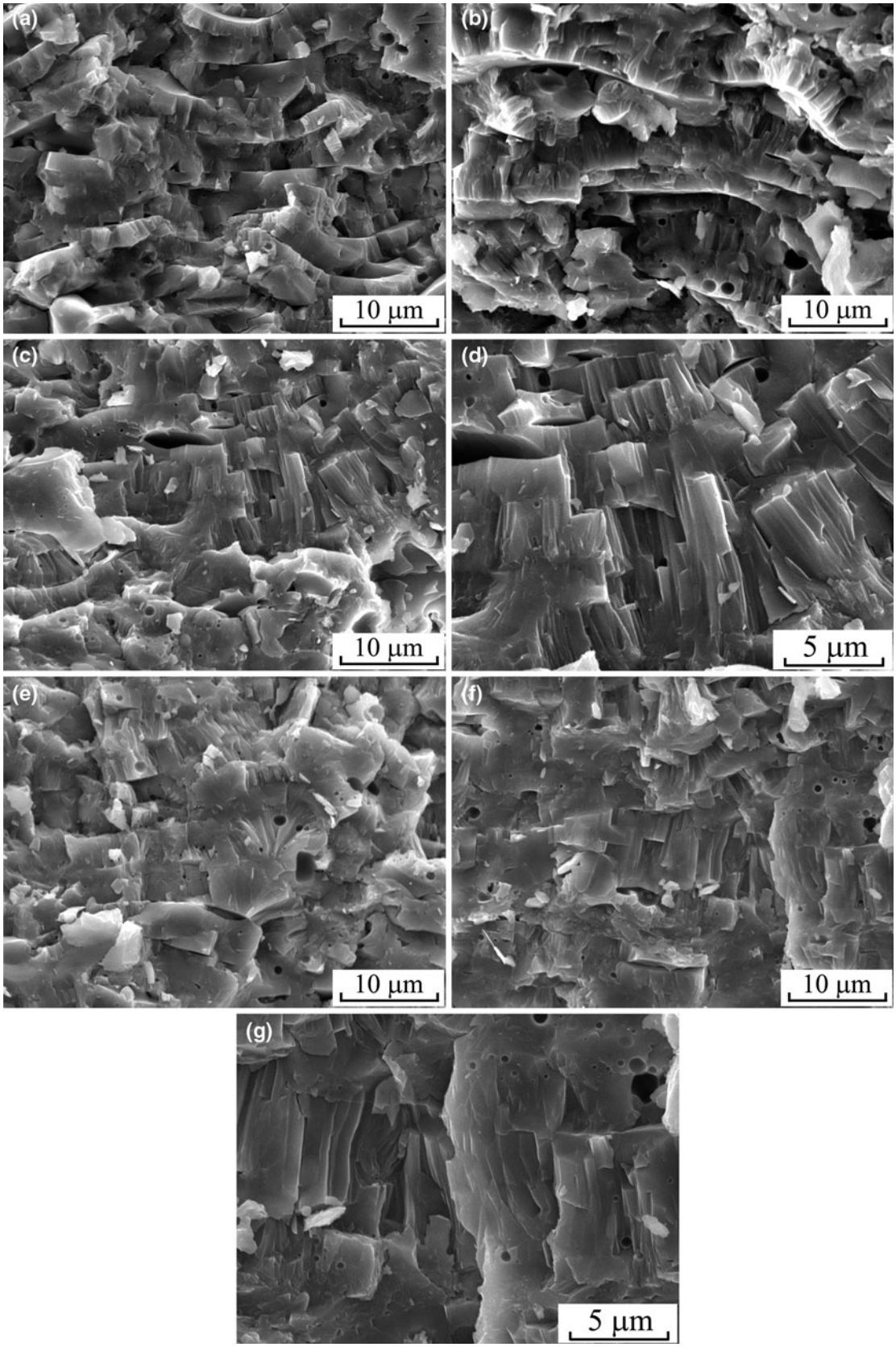

Fig. 2 Morphology of the fractured Al_2O_3 coatings plasma-sprayed at different deposition temperatures observed by SEM showing the change of the inter-lamellar bonding with the deposition temperature: (a) 140 °C, (b) 275 °C, (c, d) 480 °C, (e) 530 °C, (f, g) 660 °C

minimum interface contact temperature at which the undercooled melt begins to solidify through grain growth on the base of the substrate grain rather than nucleation for different materials.

Based on the previous systematical investigations (Ref 8, 18), it was suggested that the low interface contact temperature and short contact time between spread molten splat and the underlying splat is responsible for the limited interface bonding. The attempt to increase the spray powder particle temperature in plasma spray process is often accompanied by the increase of particle velocity and subsequently the decrease of particle heating time by plasma flame. Moreover, the need to supply the heat of fusion makes most spray particles remain at the melting point for a relatively large proportion of their residence time in the plasma flame (Ref 36). Accordingly, the improved heating of plasma flame to spray particles mainly contributes to the increase of the amount of spray particles which achieve the sufficient melting to a temperature at the melting point (Ref 36). As a result, the maximum bonding ratio was saturated to be about 32% despite of the increase of plasma arc power as reported in the previous report (Ref 8, 9, 18). It is obvious that the interface contact temperature between spread molten splat and the underlying splat increases with the increase of the underlying splat surface temperature. Therefore, as an alternative approach to increase the contact temperature between spread molten particle and the underlying splat, increasing coating surface temperature has been proposed in the previous reports (Ref 17). The present results provide further evidence to prove the above-mentioned approach to be effective to increase the lamellar interface bonding. However, the question is how and why the rapid cooling splat melt is bonded to the underlying splat. The experimental observation clearly indicates that the bonding is realized through columnar grain growth, i.e., heterogeneous nucleation using substrate surface grains, i.e. previously deposited splats, as the nucleus seeds.

When a molten spray droplet impacts on the splat surface which is maintained at an increased temperature, the increment of the contact temperature is possibly proportional to the increased surface temperature due to the rise of initial surface temperature level in the temperature range of this study (Ref 37). The increased contact temperature possibly leads to the increase of the wettability of spread melt to the underlying solid splat. Because most alumina spray particles prior to impact were at a temperature of the melting point as mentioned above, the alumina substrate surface could not be heated to fusion by the heat supplied by molten alumina particle. Therefore, it can be considered that the lamellar interface bonding involves the wetting of spread molten splat to the solid splat surface. The wettability is thus increased with the increase of coating surface temperature. Due to the less possibility of melting of the substrate surface layer by its identical melt thin layer at the melting point, the full understanding of the bonding mechanism involves the wetting of a melt material near its melting point to its identical material at the solid state. Therefore, further study into the wettability of the undercooling melt with its identical solid material will benefit deeper understanding of bonding formation mechanisms.

The polished cross-sectional microstructures of coatings deposited at different deposition temperatures are shown in Fig. 3. Pores were observed on cross sections and evidently decreased with the increase of the deposition temperature. Two kinds of pores were present in the cross sections, the pull-out of the weakly bonded splats in the coatings and the pores formed during the deposition process. It can be clearly observed that many spherical voids were present on the fracture surface of the coating besides the nonbonded interface area as clearly shown in Fig. 2(b), (d), and (e). Evidently, many spherical voids are present in individual single splat layers as seen in Fig. 2(g). This fact suggests that such voids resulted from gas which is possibly absorbed during in-flight or entrapped upon impact; although, further investigation may be necessary to examine the formation of such spherical voids. Figure 4 shows the apparent porosity levels of the coatings, which were determined by image analyzing using the polished cross-sectional microstructures. It is clear that the apparent porosity decreases with the increase of the deposition temperature. This fact is consistent with that reported by Sarikara (Ref 16). When the deposition temperature increased from 140 to 660 °C, the mean apparent porosity of the coatings decreased from 16.7 to 8.5%.

Studies have revealed that the mean bonding ratio at the interfaces between lamellae is less than 1/3 of the total apparent interface area for Al_2O_3 coating deposited with the deposition temperature maintained at a low level (Ref 7-9). The present results indicate evidently that increasing the deposition temperature promotes the growth of columnar grains across splat-splat interface, which leads to the increase of the mean interface bonding ratio and the coating density as well.

As the mean bonding ratio is the most important factor in controlling deposit properties, such as Young's modulus, fracture toughness, thermal conductivity, and so on (Ref 9), the increased bonding ratio through the columnar grain growth should lead to significant changes of coating properties.

3.2 Effect of the Deposition Temperature on the Crystalline Structure of Al_2O_3 Coating

The XRD analyses were carried out at the surface of as-sprayed coatings. The XRD patterns of Al_2O_3 coatings deposited at different deposition temperatures are shown in Fig. 5. It is clear that γ-Al_2O_3 is the main phase formed in the coatings deposited in this study besides a certain amount of α-Al_2O_3. It is well known that plasma-spraying of Al_2O_3 generally results in the formation of metastable γ-Al_2O_3 in the coating due to rapid solidification of alumina splats during splat cooling, and the presence of α-Al_2O_3 phase is due to the inclusion of unmelted fraction in partially melted Al_2O_3 particles into coatings. A change in the spray conditions changes the γ to α ratio (Ref 38, 39). The contents of α- and γ-Al_2O_3 phases in the coatings were estimated based on the relative intensity of

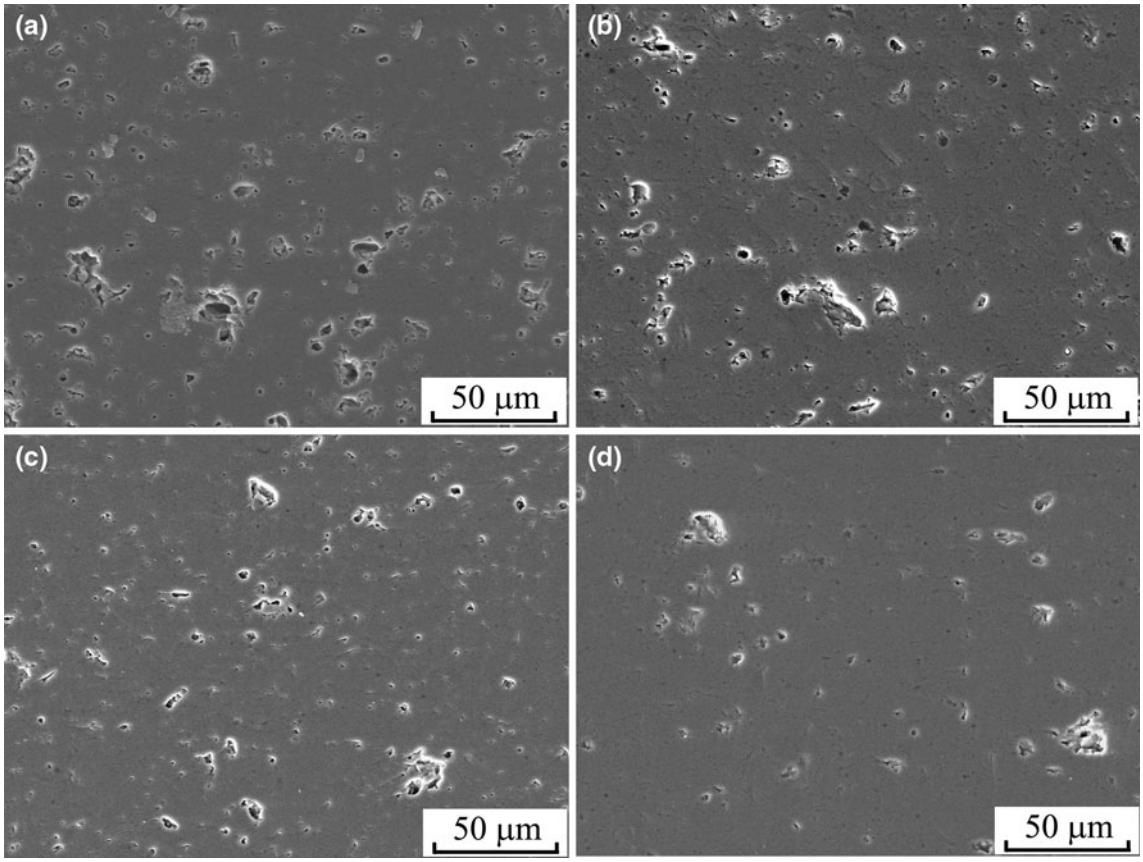

Fig. 3 Cross-sectional SEM microstructure of polished Al_2O_3 coatings plasma-sprayed at different deposition temperatures: (a) 140 °C, (b) 480 °C, (c) 530 °C, (d) 660 °C

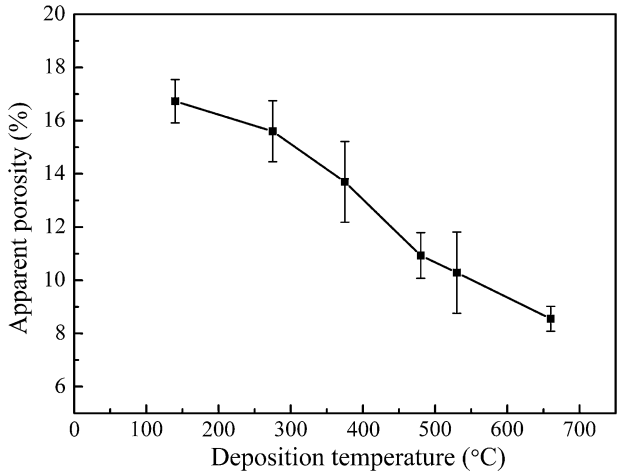

Fig. 4 The effect of the deposition temperature on the apparent porosity of plasma-sprayed Al_2O_3 coatings

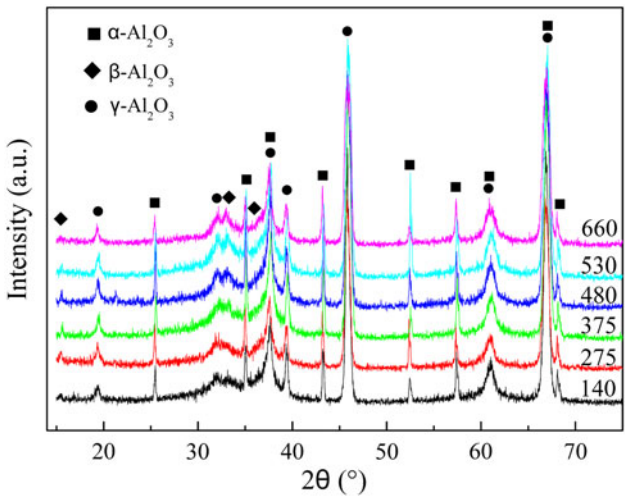

Fig. 5 XRD patterns of Al_2O_3 coatings plasma-sprayed at different deposition temperatures

the main peaks of α-Al_2O_3 and γ-Al_2O_3 in XRD patterns (Ref 31, 32), and the results are shown in Table 2. β-Al_2O_3 in the coating was neglected due to limited amount. It can be seen that the phase content changed less significantly at the deposition temperature range in this study. Heintze and Uematsu (Ref 23) investigated the effect of substrate temperature on the phase evolution during plasma spraying of Al_2O_3 and reported that the formation of α-Al_2O_3 as the primary phase occurs at a substrate temperature of 1300 °C.

Table 2 Phase content of alumina coatings plasma-sprayed at different deposition temperatures

Deposition temperature, °C	Phase content, %	
	α-Al_2O_3	γ-Al_2O_3
140	19.9	80.1
275	26.4	73.6
375	24.6	75.4
480	25.1	74.9
530	25.5	74.5
660	24.2	75.8

3.3 Influence of the Deposition Temperature on Properties of Coatings

Properties of a material depend on its microstructure. In this study, the deposition temperature was employed as a key parameter to modify the microstructure of Al_2O_3 coatings deposited by plasma spraying. From the XRD analysis of the coatings, it is clear that no significant change in the phase content occurs among the coatings deposited at different temperatures in this study. The only change in the coatings deposited at different temperatures was the change of the mean lamellar interface bonding which results from the columnar grain growth across multi-splats, and the apparent porosity. Accordingly, the coating properties will change with the change of the coating lamellar microstructure and interface bonding ratio.

3.3.1 Effect of the Deposition Temperature on Coating Micro-Hardness. The micro-hardness of Al_2O_3 coatings deposited at different temperatures is shown in Fig. 6. It is obvious that the micro-hardness of coatings increased with the increase of the deposition temperature. With the coating deposited at ambient atmosphere, Al_2O_3 exhibits a mean hardness of 927 Hv. This value is consistent with those reported in literature (Ref 40). Micro-hardness values of Al_2O_3 coatings increased from 927 to 1320 $Hv_{0.3}$, while the mean deposition temperature changed from 140 to 660 °C.

Hardness is a measure of a material's resistance to plastic deformation. From the microstructure of the coating deposited at about 140 °C (Fig. 2a), the coating presents a typical lamellar structure with a limited lamellar interface bonding. The mean apparent porosity of the coating is also high. The limited interface bonding of the coating with lamellar structure leads to its low resistance to plastic deformation. When Al_2O_3 coatings were deposited at a temperature higher than 375 °C, the columnar grain growth across several splats occurs in coatings (Fig. 2c-j). The growth of columnar grains across splat-splat interface leads to increase of the interface bonding ratio and subsequently the density. Accordingly, the higher micro-hardness value is associated with the improved lamellar interface bonding.

3.3.2 Effect of the Deposition Temperature on Young's Modulus of Al_2O_3 Coating. The Knoop indentation method (Ref 22, 23) was employed to measure the Young's modulus of the coatings deposited at different temperatures. The cross sections were pre-polished and used to indent the Knoop indentation. The test was performed at a load of 1000 gf and loading time of 50 s to ensure a sufficient deformation of the coating to yield at the direction perpendicular to lamellae. Accordingly, Young's modulus obtained is that for the direction perpendicular to lamellar interface. The Young's modulus of Al_2O_3 coatings deposited at different temperatures is shown in Fig. 7. Obviously, the Young's modulus of coatings increases with the increase of the deposition temperature. Young's modulus values changed from 107 to 166 GPa, being increased by a factor of 55%, when the deposition temperature changed from 140 to 660 °C.

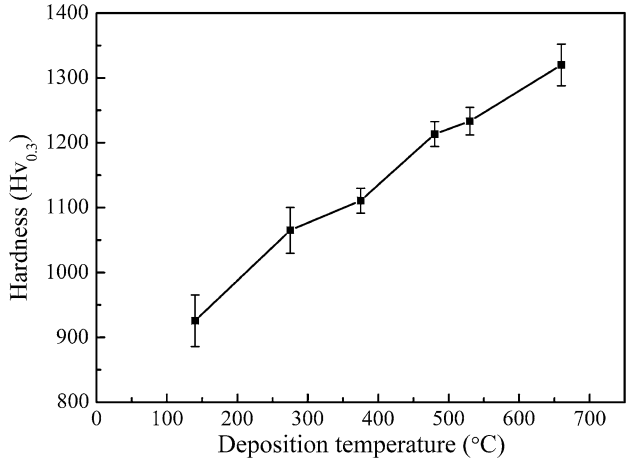

Fig. 6 The effect of the deposition temperature on micro-hardness of Al_2O_3 coatings

It is known that thermally sprayed coatings exhibit lower Young's modulus than corresponding bulk materials, which is significantly influenced by the limited interface bonding (Ref 11-13). While, the measured values may depend on the spraying methods and conditions, as well as the measuring methods (Ref 41-43). Kawase et al. (Ref 41) investigated the Young's modulus of detonation-gun and plasma-sprayed Al_2O_3 coatings using the four-point bending test, x-ray method, and ultrasonic method. The Young's modulus of detonation-gun coatings are 110-120 GPa measured by the four-point bending test, and 60-70 GPa measured by the ultrasonic method. However, the Young's modulus of the plasma-sprayed coatings are 20-50 GPa measured by the ultrasonic method. Moreover, with Young's modulus of plasma-sprayed Al_2O_3 coatings Shi et al. (Ref 42) reported 60-90 GPa, measured by the four-point bending test, and Yamasaki and Takeuchi (Ref 43) reported 95.6 GPa, measured by the resonating method. Accordingly, in the present investigation, the measurement of Young's modulus of plasma-sprayed Al_2O_3 coating deposited at 140 °C yielded 107 GPa by the Knoop indentation method, which is consistent with the highest value among the reported values.

According to the previous studies (Ref 9, 13), the Young's modulus of plasma-sprayed ceramic coating is determined by the lamellar interface bonding ratio and the

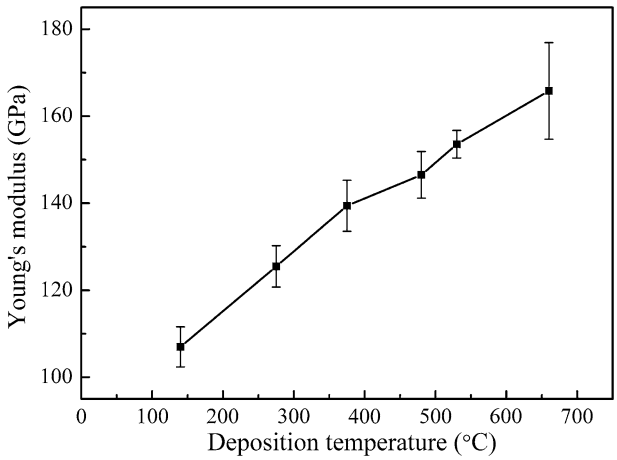

Fig. 7 The effect of the deposition temperature on the Young's modulus of Al_2O_3 coatings

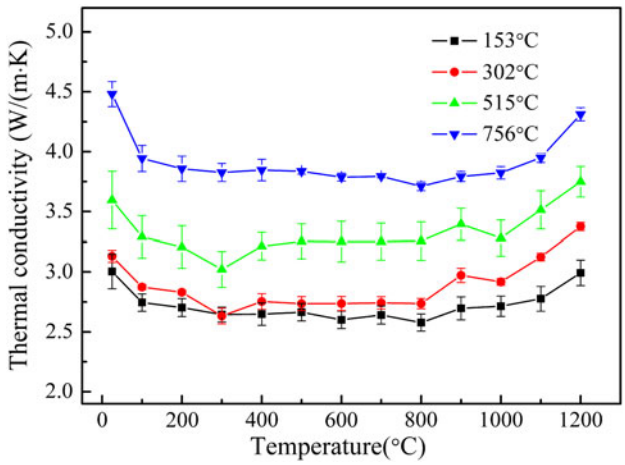

Fig. 8 Thermal conductivities of Al_2O_3 coatings sprayed at different temperatures against test temperature

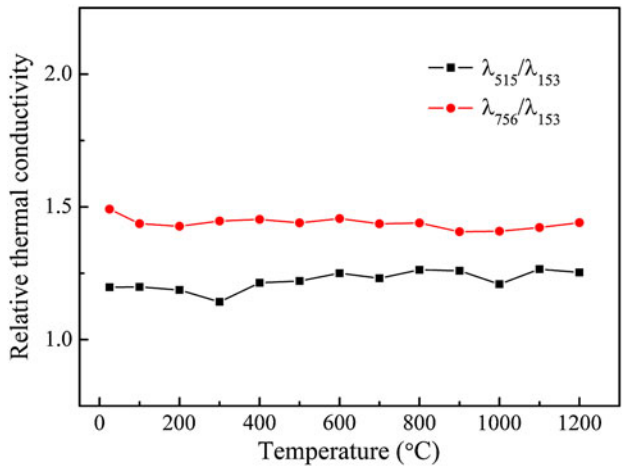

Fig. 9 Relative thermal conductivities of plasma-sprayed Al_2O_3 coatings against test temperature

modulus of lamella material as the bonding ratio is higher than about 40%. Plasma-sprayed Al_2O_3 coating consists mainly of γ-Al_2O_3, the Young's modulus of which was not known yet. Based on the previous study (Ref 13), the Young's modulus of γ-Al_2O_3 was estimated to be about 246 GPa, while the Young's modulus of α-Al_2O_3 is 380 GPa. According to phase contents shown in Table 2, the modulus of individual lamellae in the coating deposited in this study is estimated of 280 GPa. As a result, the apparent interface bonding ratio could be estimated to be 38 and 59.3% for the coatings deposited at 140 and 660 °C.

3.3.3 Effect of the Deposition Temperature on the Thermal Conductivity of Al_2O_3 Coating. The thermal conductivity of Al_2O_3 coatings deposited at different temperatures is shown in Fig. 8. The thermal conductivity was plotted against test temperature during measurement. It is clear that the thermal conductivity of plasma-sprayed Al_2O_3 coatings increased with the increase of the deposition temperature.

With thermally sprayed ceramic coatings, the microstructure of the deposit significantly influences its thermal transportation. Previous studies have shown that the limited bonding at the lamellar interfaces in ceramic coatings leads to much lower thermal conductivity than bulk dense material (Ref 15). For bulk dense Al_2O_3, the thermal conductivity ranges from 29 to 36 W/(m · K) at 300 K (Ref 44). Pawlowski and Fauchais (Ref 45) reviewed the thermal properties of thermally sprayed coatings, and the thermal conductivity of plasma-sprayed Al_2O_3 coating ranges from 2 to 3 W/(m · K) at 473-1180 K. Dutton et al. (Ref 46) reported that the thermal conductivity of plasma-sprayed Al_2O_3 coating ranges from 1.5 to 3 W/(m · K) at room temperature to 1000 °C. Based on the present investigation, the thermal conductivity of plasma-sprayed Al_2O_3 coating deposited at 153 °C ranges from 2.5 to 3 W/(m · K) at 25-1200 °C. These values are consistent with those reported in literature (Ref 45, 46).

As estimated from the measurement of Young's modulus mentioned in the previous section, when the deposition temperature was increased to 660 °C, the lamellar interface bonding ratio is significantly increased. Thermal conductivity measured at a temperature of 600 °C changed from 2.6 to 3.9 W/(m · K), being increased by a factor of 50%, when the mean deposition temperature was increased from 153 to 756 °C. It can be recognized that this fraction of the increment is close to 55% observed for Young's modulus in the temperature range of 140 to 660 °C. The relative thermal conductivity of coatings deposited at 756 to 153 °C, and 515 to 153 °C is shown in Fig. 9. It can be clearly recognized that despite significant change of thermal conductivity with test temperature, the relative conductivity at two different deposition temperatures is nearly a constant. Such constant is considered to be equal to the increased fraction of the lamellar interface bonding ratio. It is clear that the relative thermal conductivity of plasma-sprayed Al_2O_3 coating deposited at 756 °C to that at 153 °C is about 1.5, being compatible to the estimated increment of the apparent lamellar bonding ratio from Young's modulus in a similar temperature range. Therefore, the increase of thermal conductivity is

evidently attributed to the increase of the lamellae interface bonding ratio.

4. Conclusions

The present results showed that the microstructure and properties of Al_2O_3 coatings were significantly influenced by the deposition temperature. As the deposition temperature was increased to above 375 °C, the columnar grain growth across splat-splat interface leading to the bonding formation at splat interfaces became remarkable. Moreover, the apparent porosity decreased and microhardness was increased with the increase of the deposition temperature. The improved lamellar interface bonding with the increase of the deposition temperature led to significant improvements of the properties of Al_2O_3 coatings. As the mean deposition temperature was increased from 140 to 660 °C and 153 to 756 °C, Young's modulus and thermal conductivity were increased by 55 and 50%, respectively. Based on the dependency of Young's modulus and thermal conductivity of plasma-sprayed ceramic coatings, it can be estimated that the mean lamellar bonding ratio was increased from 32 to 38% and 59.3% when the deposition temperature was increased from near-room temperature to 140 and 660 °C, respectively.

Acknowledgment

The present research project is supported by National Science Fund for Distinguish Young Scholars of China (Granted No. 50725101).

References

1. P. Fauchais, A. Vardelle, and B. Dussoubs, Quo Vadis Thermal Spraying?, *J. Thermal Spray Technol.*, 2001, **10**(1), p 44-66
2. E. Lugscheider, C. Barimani, P. Eckert, and U. Eritt, Modeling of the APS Plasma Spray Process, *Comput. Mater. Sci.*, 1996, **7**(1-3), p 109-114
3. B. Goswami, A.K. Ray, and S.K. Sahay, Thermal Barrier Coating System for Gas Turbine Application—A Review, *High Temp. Mater. Process.*, 2004, **23**(2), p 73-92
4. M. Mohanty and R.W. Smith, Lightweight TiC/Ti Wear-resistant Coatings for Lightweight Structural Applications, *J. Thermal Spray Technol.*, 1995, **4**(4), p 384-394
5. H. Singh, B.S. Sidhu, D. Puri, and S. Prakash, Use of Plasma Spray Technology for Deposition of High Temperature Oxidation Corrosion Resistant Coatings—A Review, *Mater. Corros.*, 2007, **58**(2), p 92-102
6. P. Ctibor, J. Sedlacek, and K. Neufuss, Influence of Chemical Composition on Dielectric Properties of Al_2O_3 and ZrO_2 Plasma Deposits, *Ceram. Int.*, 2003, **29**(5), p 527-532
7. A. Ohmori and C.-J. Li, Quantitative Characterization of the Structure of Plasma Sprayed Al_2O_3 Coating by Using Copper Electroplating, *Thin Solid Films*, 1991, **201**(2), p 241-252
8. A. Ohmori, C.-J. Li, and Y. Arata, Structure of Plasma-sprayed Alumina Coatings Revealed by Using Copper Electroplating, *Proceedings of the 4th National Thermal Spray Conference, Thermal Spray Coatings: Properties, Processes and Applications*, T.F. Bernecki, Ed., May 4-10, 1991 (Pittsburgh, PA), ASM International, 1992, p 105-113
9. C.-J. Li and A. Ohmori, Relationships Between the Microstructure and Properties of Thermally Sprayed Deposits, *J. Thermal Spray Technol.*, 2002, **11**(3), p 365-374
10. Z.J. Yin, S.Y. Tao, X.M. Zhou, and C.X. Ding, Evaluating Microhardness of Plasma Sprayed Al_2O_3 Coatings Using Vickers Indentation Technique, *J. Phys. D Appl. Phys.*, 2007, **40**(22), p 7090-7096
11. R. McPherson and B.V. Shafer, Interlamellar Contact Within Plasma-sprayed Coatings, *Thin Solid Films*, 1982, **97**(3), p 201-204
12. S. Kuroda and T.W. Clyne, The Quenching Stress in Thermally Sprayed Coatings, *Thin Solid Films*, 1991, **200**(1), p 49-66
13. C.-J. Li, A. Ohmori, and R. McPherson, The Relationship Between Microstructure and Young's Modulus of Thermally Sprayed Ceramic Coatings, *J. Mater. Sci.*, 1997, **32**(4), p 997-1004
14. C.-J. Li, W.-Z. Wang, and H. Yong, Dependency of Fracture Toughness of Plasma Sprayed Al_2O_3 Coatings on Lamellar Structure, *J. Thermal Spray Technol.*, 2004, **13**(3), p 425-431
15. R. McPherson, A Model for the Thermal Conductivity of Plasma-Sprayed Ceramic Coatings, *Thin Solid Films*, 1984, **112**(1), p 89-95
16. O. Sarikaya, Effect of the Substrate Temperature on Properties of Plasma Sprayed Al_2O_3 Coatings, *Mater. Des.*, 2005, **26**(1), p 53-57
17. Y.-Z. Xing, C.-J. Li, C.-X. Li, and G.-J. Yang, Influence of Through-lamella Grain Growth on Ionic Conductivity of Plasma-sprayed Yttria-stabilized Zirconia as an Electrolyte in Solid Oxide Fuel Cells, *J. Power Sour.*, 2008, **176**(1), p 31-38
18. A. Ohmori, C.J. Li, and Y. Arata, Influence of Plasma Spray Conditions on the Structure of Al_2O_3 Coatings, *Trans. Jpn. Weld. Res. Inst.*, 1990, **19**, p 259-270
19. Z.J. Yin, S.Y. Tao, X.M. Zhou, and C.X. Ding, Particle in-flight Behavior and Its Influence on the Microstructure and Mechanical Properties of Plasma-Sprayed Al_2O_3 Coatings, *J. Eur. Ceram. Soc.*, 2008, **28**(6), p 1143-1148
20. J.R. Mawdsley, Y.J. Su, and K.T. Faber, Optimization of Small-particle Plasma-Sprayed Alumina Coatings Using Designed Experiments, *Mater. Sci. Eng. A*, 2001, **308**(1-2), p 189-199
21. L. Bianchi, A.C. Leger, M. Vardelle, A. Vardell, and P. Fauchais, Splat Formation and Cooling of Plasma-Sprayed Zirconia, *Thin Solid Films*, 1997, **305**(1), p 35-47
22. V. Pershin, M. Lufitha, S. Chandra, and J. Mostaghimi, Effect of Substrate Temperature on Adhesion Strength of Plasma-Sprayed Nickel Coatings, *J. Thermal Spray Technol.*, 2003, **12**(3), p 370-376
23. P. Fauchais, M. Fukumoto, M. Vardelle, and A. Vardell, Knowledge Concerning Splat Formation: An Invited Review, *J. Thermal Spray Technol.*, 2004, **13**(3), p 337-360
24. G.N. Heintze and S. Uematsu, Preparation and Structures of Plasma-Sprayed γ- and α-Al_2O_3 Coatings, *Surf. Coat. Technol.*, 1992, **50**(3), p 213-222
25. I.H. Jung, K.K. Bae, M.S. Yang, and S.K. Ihm, A Study of the Microstructure of Yttria-Stabilized Zirconia Deposited by Inductively Coupled Plasma Spraying, *J .Thermal Spray Technol.*, 2000, **9**(4), p 463-477
26. H.B. Guo, R. Vassen, and D. Stöver, Atmospheric Plasma Sprayed Thick Thermal Barrier Coatings with High Segmentation Crack Density, *Surf. Coat. Technol.*, 2004, **186**(3), p 353-363
27. H.B. Guo, S. Kuroda, and H. Murakami, Microstructures and Properties of Plasma-Spayed Segmented Thermal Barrier Coatings, *J. Am. Ceram. Soc.*, 2006, **89**(4), p 1432-1439
28. H.B. Guo, S. Kuroda, and H. Murakami, Segmented Thermal Barrier Coatings Produced by Atmospheric Plasma Spraying Hollow Powders, *Thin Solid Films*, 2006, **506-507**, p 136-139
29. A. Tricoire, M. Vardelle, P. Fauchais, F. Braillard, A. Malie, and P. Bengtsson, Macrocrack Formation in Plasma-Sprayed YSZ TBCs when Spraying Thick Passes, *High Temp. Mater. Process.*, 2005, **9**, p 401-413
30. Y.-Z. Xing, Y. Li, C.-J. Li, C.-X. Li, and G.-J. Yang, Influence of Substrate Temperature on Microcracks Formation in Plasma-Sprayed Yttria-Stabilized Zirconia Splats, *Key Eng. Mater.*, 2008, **373-374**, p 69-72

31. S. Hillier, Accurate Quantitative Analysis of Clay and other Minerals in Sandstones by XRD: Comparison of a Rietveld and a Reference Intensity Ratio (RIR) Method and the Importance of Sample Preparation, *Clay Miner.*, 2000, **35**(1), p 291-302
32. Q. Johnson and R.S. Zhou, Checking and Estimating RIR Values, *Adv. X-ray Anal.*, 2000, **42**, p 287-296
33. D.B. Marshall, T. Noma, and A.G. Evans, A Simple Method for Determining Elastic-Modulus-to-Hardness Ratios Using Knoop Indentation Measurements, *J. Am. Ceram. Soc.*, 1982, **65**(10), p 175-176
34. F. Kroupa and J. Dubsky, Pressure Dependence of Young's Modulus of Thermal Sprayed Materials, *Scr. Mater.*, 1999, **40**(11), p 1249-1254
35. Y.-Z. Xing, C.-J. Li, Q. Zhang, C.-X. Li, and G.-J. Yang, Influence of Microstructure on the Ionic Conductivity of Plasma-Sprayed Yttria-Stabilized Zirconia Deposits, *J. Am. Ceram. Soc.*, 2008, **91**(12), p 3931-3936
36. A. Vardelle, M. Vardelle, R. McPherson, and P. Fauchais, Study of the Influence of Particle Temperature and Velocity Distribution within a Plasma Jet Coating Formation, *General Aspect of Thermal Spraying* (*Proceedings of 9th International Thermal Spray Conference*), The Hague, 19-23 May 1980, pp 155-161
37. Y.-Z. Xing, C.-J. Li, J.-H. Qiao, and G.-X. Wang, Analysis on Rapid Cooling and Epitaxial Solidification of a Plasma-sprayed Yttria Stabilized Zirconia Splat on a High-temperature Substrate, *Proceedings of the ASME International Mechanical Engineering Congress and Exposition*, 2008, Vol. 8, pts A and B, p 1837-1844
38. M. Vardelle and J.L. Besson, γ-Alumina Obtained by Arc Plasma Spraying: A Study of the Optimization of Spraying Conditions, *Ceram. Int.*, 1981, **7**(2), p 48-54
39. P. Chraska, J. Dubsky, and K. Neufuss, Alumina-Base Plasma-Sprayed Materials, Part I: Phase Stability of Alumina and Alumina-Chromia, *J. Thermal Spray Technol.*, 1997, **6**(3), p 320-326
40. Y.Arata, A.Ohmori, and C.-J. Li, Fundamental Properties of the ACT-JP (Arata Coating Test with Jet Particles), *Proceedings of the 1st National Thermal Spray Conference, Thermal Spray: Advances in Coatings Technology*, D.L. Houck, Ed., Sept 14-17, 1987 (Orlando, FL), ASM International, 1988, p 79-83
41. R. Kawase, K.Tanaka, T. Hamamoto, and H. Haraguchi, Study on Elastic Constant and Residual Stress Measurements during Ceramic Coatings, *Proceedings of the 3rd National Thermal Spray Conference, Thermal Spray Research and Applications*, T.F. Bernecki, Ed., May 20-25, 1990 (Long Beach, CA), ASM International, 1991, p 339-342
42. K.S. Shi, Z.Y. Qian, and M.S. Zhang, Microstructure and Properties of Sprayed Ceramic Coating, *J. Am. Ceram. Soc.*, 1988, **71**(11), p 924-929
43. R. Yamasaki and J. Takeuchi, Physical Characteristics of Alumina Coating Using Atmospheric Plasma Spraying(APS) and Low Pressure Plasma Spraying(VPS), *Proceeding of the International Thermal Spray Conference, Thermal Spray 2004: Advances in Technology and Application*, ASM International, May 10-12, 2004 (Osaka, Japan), ASM International, 2004, p 283-289
44. J. Francel and W.D. Kingrey, Thermal Conductivity: IV, Apparatus for Determining Thermal Conductivity by a Comparative Method, *J. Am. Ceram. Soc.*, 1954, **37**(2), p 80-81
45. L. Pawlowski and P. Fauchais, Thermal Transport Properties of Thermally Spayed Coatings, *Int. Mater. Rev.*, 1992, **37**, p 271-289
46. R. Dutton, R. Wheeler, K.S. Ravichandran, and K. An, Effect of Heat Treatment on the Thermal Conductivity of Plasma-Sprayed Thermal Barrier Coatings, *J. Thermal Spray Technol.*, 2000, **9**(2), p 204-209